The Journal of Immunology

Processing of an Antigenic Sequence from IgG Constant Domains for Presentation by MHC Class II

Morten Flobakk, Ingunn B. Rasmussen, Elin Lunde, Terje Frigstad, Gøril Berntzen, Terje E. Michaelsen, Bjarne Bogen and Inger Sandlie

J Immunol 2008; 181:7062-7072; ;
doi: 10.4049/jimmunol.181.10.7062
http://www.jimmunol.org/content/181/10/7062

The Journal of Immunology is published twice each month by
The American Association of Immunologists, Inc.,
9650 Rockville Pike, Bethesda, MD 20814-3994.

Print ISSN: 0022-1767 Online ISSN: 1550-6606.

Processing of an Antigenic Sequence from IgG Constant Domains for Presentation by MHC Class II[1]

Morten Flobakk,[2]*‡ Ingunn B. Rasmussen,*‡ Elin Lunde,*‡ Terje Frigstad,†‡ Gøril Berntzen,*‡ Terje E. Michaelsen,§ Bjarne Bogen,†‡ and Inger Sandlie[3]*‡

Targeting of T cell epitopes to APC enhances T cell responses. We used an APC-specific Ab (anti-IgD) and substituted either of 18 loops connecting β strands in human IgG constant H (C_H) domains with a characterized T cell peptide epitope. All Ab-epitope fusion molecules were secreted from producing cells except IgG-loop 2(BC)C_H1, and comparing levels, a hierarchy appeared with fusions involving $C_H2 \geq C_H1 > C_H3$. Within each domain, fusion at loop 6(FG) showed best secretion, while low secretion correlated with the substitution of native loops that contain conserved amino acids buried within the folded molecule. Comparing the APC-specific rAb molecules for their ability to induce T cell activation in vitro, the six mutants with epitope in C_H2 were the most effective, with loop 4C_H2 ranking on top. The C_H1 mutants were more resistant to processing, and the loop 6C_H1 mutant only induced detectable activation. The efficiency of the C_H3 mutants varied, with loop 6C_H3 being the least effective and equal to loop 6 C_H1. Considering both rAb secretion level and T cell activation efficiency, a total of eight loops may carry T cell epitopes to APC for processing and presentation to T cells, namely, all in C_H2 in addition to loop 6 in C_H1 and C_H3. Comparing loop 4C_H2 with loop 6C_H1 mutants after injection of Ab in BALB/c mice, the former was by far the most efficient and induced specific T cell activation at concentrations at least 100-fold lower than loop 6C_H1. ***The Journal of Immunology,*** **2008, 181: 7062–7072.**

Increased presentation of antigenic peptide in complex with MHC molecules enhances T cell responses, and Ab- mediated targeting of peptide or whole Ag to APC is a way to increase the number of peptide-MHC complexes on the surface of APC (1). This is important since major efforts are concentrated on the development of safe vaccines that generate strong, specific T cell responses. Abs with T cell epitopes within their V region CDR loops have been described previously (2). Although such rAbs may enter APC by way of FcγRs, rAbs with peptides or whole Ag added C-terminally to Fab (3) or to Ab (4, 5) may target a preferred and defined APC surface molecule by way of V region specificity. We have introduced peptide epitopes into loops connecting β strands in constant heavy (C_H)[4] domains, and denoted the epitope-loaded rAb "Troybodies." The loop-grafting experiments have involved the amino acid sequence 91–101 of the MOPC315 plasmacytoma λ2 L chain (91–101 $\lambda2^{315}$), which represents a minimal stimulating T cell epitope (6) presented on I-E^d MHC class II for $CD4^+$ T cells (7). In initial experiments, this epitope was exchanged with or inserted into either of three loops (BC, DE, or FG) in C_H1 of human (h) IgG3 (8) and murine (m) IgG2b (9). For simplicity, these loops are hereby denoted loop 2C_H1, 4C_H1, and 6C_H1, respectively (see Fig. 1*A*). The loop 2C_H1 hIgG3 rAb mutant was retained, while all other single loop substitution mutants were secreted. We also showed that loop 6C_H1 hIgG3 could be substituted with model epitopes that show great variation in amino acid sequence, length, and secondary structure, namely, aa 323–339 from OVA, aa 110–120 from hemagglutinin, and aa 46–61 from hen egg lysozyme (10). Initially, the epitope was grafted into hapten-specific rAbs (8) and, subsequently, the rAbs were equipped with V genes encoding APC specificity. Following in vitro targeting, the epitopes were excised from the rAbs, loaded on MHC class II molecules, and presented to specific T cells. Such Troybody targeting to murine IgD^a resulted in a 10^3-fold improvement in presentation efficiency compared with rAbs with irrelevant specificity. Importantly, T cell activation was improved up to 10^5-fold compared with that achieved using synthetic peptide or whole protein (10, 11). The same results were obtained in experiments with (91–101 $\lambda2^{315}$) in loop 6C_H1 where the target was MHC class II (I-E) (12). Furthermore, a 10^2-fold enhanced presentation was seen in vivo in mice (12).

Comparing the in vitro presentation efficiency of APC loaded with mouse and human rAbs with 91–101 $\lambda2^{315}$epitopes grafted in various loops in C_H1 (8, 9), differences were found which prompted us to initiate a comprehensive analysis that involved grafting in all loops in all three C_H domains. Each domain has six loops connecting β strands, offering 18 possibilities for loop replacement. To identify the loops that are best suited for epitope insertion, we exchanged every loop in the three hIgG3 C_H domains with the amino acid sequence 89–105 from $\lambda2^{315}$ (89–105) $\lambda2^{315}$ and show here that a total of 17 such fusion molecules were secreted from transiently transfected 293E cells, although in different amounts. Levels of secretion are compared with variability as well as hydropathicity and solvent accessibility score for each amino acid within each domain.

For each domain, the loop 6 mutant was secreted at the highest level. Furthermore, the C_H1 and C_H2 mutants (except loop 2C_H1)

*Department of Molecular Biosciences, †Institute of Immunology, and ‡Centre for Immune Regulation, University of Oslo, Oslo, Norway; and §Department of Vaccines, National Institute of Public Health, Oslo, Norway

Received for publication July 11, 2007. Accepted for publication September 6, 2008.

The costs of publication of this article were defrayed in part by the payment of page charges. This article must therefore be hereby marked *advertisement* in accordance with 18 U.S.C. Section 1734 solely to indicate this fact.

[1] This work was funded by the Norwegian Cancer Society (to M.F. and I.B.R.) and the Research Council of Norway (to E.L., T.F., and G.B.).

[2] Current address: BioInn, 2317 Hamar, Norway.

[3] Address correspondence and reprint requests to Dr. Inger Sandlie, Department of Molecular Biosciences, University of Oslo, PO Box 1041 Blindern, NO-0316 Oslo, Norway. E-mail address: inger.sandlie@imbv.uio.no.

[4] Abbreviations used in this paper: C_H, constant region of Ig H chain; RT, room temperature; AEP, asparaginyl endopeptidase; wt, wild type.

were secreted better than the C_H3 domain mutants, of which the loop 6 mutant only was secreted well. In general, low secretion correlated with the removal of conserved amino acids that were buried either within a domain core or between two interacting domains.

All secreted rAbs were tested for the ability to stimulate $CD4^+$ T cells in vitro in T cell activation and growth inhibition assays. Importantly, T cell epitope loop grafting on all three C_H domains was compatible with efficient stimulation of T cells. Eight mutants were both secreted in good amounts and found to induce T cell activation, namely, loop $6C_H1$, all C_H2 mutants and loop $6C_H3$. The difference in induction potential was large, as the best activator (loop $4C_H2$) induced T cell activation at a concentration that was 10^2-fold lower than the weakest (loop $6C_H1$). These two Abs were selected for further studies in vivo and both were injected into the tail vein of normal mice at various concentrations. Following in vivo targeting, isolated spleen cells as APC stimulated specific T cells in vitro and again the loop $4C_H2$ mutant was at least 10^2-fold more efficient than the loop $6C_H1$ mutant.

Table I. *Loop positions in hIgG3*

Domain	Loop[a]	EU No.
C_H1	1	129–138
	2	150–153
	3	159–166
	4	175–179
	5	189–196
	6	205–208
C_H2	1	244–257
	2	265–273
	3	280–289
	4	296–299
	5	308–318
	6	325–331
C_H3	1	352–361
	2	371–377
	3	384–390
	4	394–405
	5	414–422
	6	429–436

[a] Loops are numbered 1–6 in each domain from the N- to the C-terminal, e.g., such that the loop connecting β strand A and B is loop 1 (Fig 1*A*).

Materials and Methods

Mice, cell lines, and Abs

BALB/c mice were bred by Taconic Farms. The study was approved by the National Committee for Animal Experiments (Oslo, Norway). 293E (CRL-10852) cells were obtained from American Type Culture Collection. The T cell clone 7A10B2 recognizes aa 91–101 of $\lambda2^{315}$ in complex with $I\text{-}E^d$ (7). Spleen cells from BALB/c mice were used as APC, as were A20 B lymphoma cells transfected with a 2,4,6-trinitrophenyl-specific IgD BCR (A20δ; gift from Dr. N. Hozumi, Department of Medical Genetics, University of Toronto, Toronto, Ontario, Canada) (13).

The 4B2A1 and 7A10B2 T cell clones recognize the same $\lambda2^{315}$ $I\text{-}E^d$ complex (7). The T cell hybridoma BW4B2A1 was produced by fusing lymph node cells from 4B2A1 TCR-transgenic SCID mice (14) with the TCR-negative T cell hybridoma line BW51.47 α/β (15) using polyethylene glycol under standard conditions. Hypoxanthine/aminopterin/thymidine-resistant clones were selected for surface expression of the 4B2A1 TCR. Functionality was confirmed by coculturing hybridoma cells with irradiated BALB/c splenocytes (20 Gy) and synthetic $\lambda2^{315}$ peptide (89–107), with subsequent detection of IL-2 in supernatant by sandwich ELISA (data not shown).

All cells were cultured in DMEM (BioWhittaker) or RPMI 1640 supplemented with 10% heat-inactivated FCS (PAA), 2 mM L-glutamine (DMEM only), 25 μg/ml streptomycin, and 25 U/ml penicillin (both from BioWhittaker) under standard conditions. Abs for IL-2 detection were rat anti-mouse IL-2 (clone JES6-1A12) and biotin rat anti-mouse IL-2 (clone JES6-5H4), both from BD Pharmingen. Abs for IFN-γ detection were rat anti-mouse IFN-γ (AN18 (16)) and biotin rat anti-mouse IFN-γ (XMG1.2-bio (17)). mAb HP-6050 is specific for hIgG3 hinge (Sigma-Aldrich). All other Abs used were produced by us using standard procedures. The mAb K13 is specific for the human κ L chain (18). The mAbs 132c8 and HP-6050 (19) were compared for binding to all four hIgG isotypes side-by-side in ELISA and found to bind the hIgG3 hinge in a similar fashion. Affinity-purified sheep polyclonal Abs, s303 (20) and s12 (21), are specific for hIgG Fab and hIgG3 hinge, respectively.

Structure analysis of hIgG3 H chain constant domains

Secondary structure analysis (β strand or loop) was conducted using data and evaluation programs given in the PDB database (http://www.rcsb.org/pdb/) (22) and as described previously (9). Briefly, crystal structures of 1FC1 (hIgG1), 1IGY (mIgG1), and 1IGT (mIgG2a) were studied regarding both loop length and limits as determined by three-dimensional visualization and the program Structure Explorer (http://www.pdb.org). Loops were numbered 1–6 in each domain starting from the N-terminal end of the polypeptide chain. Variability of each amino acid position in Ig H chains was analyzed using the sequence analysis program provided by S. M. J. Searle (The Sanger Institute, Cambridge, U.K.) as described previously (9).

The relative total side chain accessibility of each amino acid in the C_H1, C_H2, and C_H3 domains was investigated using Naccess (http://wolf.bms.umist.ac.uk/naccess/) and PDB ID: 1HZH (human IgG1) (23). Hydropathicity analysis of hIgG3 domains C_H1, C_H2, and C_H3 was performed using the program ProtScale (window size = 9; http://www.expasy.org/cgi-bin/protscale.pl) (24) and the Kyte-Doolittle scale (25), as provided by the Swiss Institute of Bioinformatics.

Production of mutant hIgG3: construction of loop exchange mutants

The C_H chain gene encoding the G3m (b0) allotype (26) was a gift from Dr. M. P. LeFranc (International ImMunoGeneTics Information System, Montpellier, France) and cloned as a 2.8-kb fragment into *Hin*dIII-*Sph*I sites in the polylinker of pUC19 (Sigma-Aldrich). The resulting plasmid, pUC19γ3wt, was template in all mutagenesis reactions. All predicted loop sequences in Cγ3 C_H1, C_H2, and C_H3, were exchanged with aa 89–105 from $\lambda2^{315}$ (FAALWFRNHFVFGGGTK) in individual H chains. The cysteine in position 90 of the endogenous sequence was exchanged with alanine. Mutagenesis was performed by QuikChange mutagenesis (Stratagene). Table I shows loop sequences and Table II shows mutagenic primer sequences. Colonies were screened for the presence of the mutation by the simultaneous introduction of a silent *Dra*III restriction site and *Dra*III digestion of plasmid DNA. All 18 mutations were subsequently confirmed by sequencing by GATC. Sequenced fragments containing mutations were subcloned into unmanipulated vectors as *Hin*dII-*Bgl*II, *Bgl*II-*Pml*I, *Pml*I-*Nsi*I, or *Pml*I-*Sph*I (Fig. 1*B*) to exclude possible amplification errors outside the sequenced areas. Complete mutant H chain genes were assembled in $pLNOH2_{IgD}$, which encode IgD-specific H chains, as described elsewhere (11, 27). The corresponding L chain gene, encoded on $pLNOK_{IgD}$ (11, 27) and each of the 18 $pLNOH2_{IgD}$ variants were transiently cotransfected in 293E cells (28). Portions of supernatant were harvested and replaced with fresh medium every 2–3 days for 14 days as described. A substitution of loop $4C_H1$ with 91–101 $\lambda2^{315}$ has been described elsewhere (8) and the complete H chain gene was assembled in $pLNOH2_{IgD}$. The corresponding loop $6C_H1$ substitution in an IgD-specific H chain has been described previously (11). Both H chain genes were transiently cotransfected with $pLNOK_{IgD}$ and supernatant harvested as described above. The complete IgD-specific rAbs are denoted "loop 4 or loop $6C_H1$ (91–101)," respectively.

Sandwich ELISA for detection of hIgG3 variant concentrations

The amounts of IgD-specific rAb mutants secreted after each transfection were measured as follows: 96-well microtiter plates were coated with a hIgG3-specific Ab and incubated overnight at room temperature (RT). Then, samples of 100 μl of diluted supernatants were added to each well and detected with a second hIgG3-specific Ab. A hIgG3wt preparation was diluted in a 3-fold series and used as standard. Three different Ab combinations were used as coat and detecting agent: s303 (2 μg/ml) and 132c8-bio (1/6000), s12 (10 μg/ml) and 132c8-bio (1/6000), as well as K13 (2 μg/ml) and s303-bio (1/6000), respectively. Detection was done with the substrate for alkaline phosphatase, *p*-nitrophenyl phosphate (Sigma-Aldrich) diluted in diethanolamine buffer to 1 mg/ml.

Table II. *Mutagenesis primers*[a]

Name	Sequence
1CH1(+)	CCCATCGGTCTTCCCCCTG**TTCGCAGCTCTATGGTTCAGAAACCACTTTGTGTTCGGTGGTGGAACCAAGACAGCGGCCCTGGGC**TGC
1CH1(−)	GCAGCCCAGGGCCGCTGT**CTTGGTTCCACCACCGAACACAAAGTGGTTTCTGAACCATAGAGCTGCGAACAGGGGGAAGACCGA**TGGG
2CH1(+)	GCTGCCTGGTCAAGGACTAC**TTCGCAGCTCTATGGTTCAGAAACCACTTTGTGTTCGGTGGTGGAACCAAG**GTGACGGTGTCGTGGAACTCA
2CH1(−)	TGAGTTCCACGACACCGTCAC**CTTGGTTCCACCACCGAACACAAAGTGGTTTCTGAACCATAGAGCTGCGAAGTAGTCCTTGAC**CAGGCAGC
3CH1(+)	ACCGGTGACGGTGTCGTGG**TTCGCAGCTCTATGGTTCAGAAACCACTTTGTGTTCGGTGGTGGAACCAAGGTGCACACCTTCCC**GGCTG
3CH1(−)	CAGCCGGGAAGGTGTGCAC**CTTGGTTCCACCACCGAACACAAAGTGGTTTCTGAACCATAGAGCTGCGAACCACGACACCGTCA**CCGGT
4CH1(+)	ACACCTTCCCGGCTGTCCTA**TTCGCAGCTCTATGGTTCAGAAACCACTTTGTGTTCGGTGGTGGAACCAAG**TACTCCCTCAGCAGCGTGGT
4CH1(−)	ACCACGCTGCTGAGGGAGTA**CTTGGTTCCACCACCGAACACAAAGTGGTTTCTGAACCATAGAGCTGCGAATAGGACAGCCGGG**AAGGTGT
5CH1(+)	TCAGCAGCGTGGTGACCGTG**TTCGCAGCTCTATGGTTCAGAAACCACTTTGTGTTCGGTGGTGGAACCAAG**ACCTACACCTGCAACGTGAATC
5CH1(−)	GATTCACGTTGCAGGTGTAGGT**CTTGGTTCCACCACCGAACACAAAGTGGTTTCTGAACCATAGAGCTGCGAA**CACGGTCACCACGCTGCTGA
6CH1(+)	CTACACCTGCAACGTGAATCAC**TTCGCAGCTCTATGGTTCAGAAACCACTTTGTGTTCGGTGGTGGAACCAAGACCAAGGTGGAC**AAGAGAGTTG
6CH1(−)	CAACTCTCTTGTCCACCTTGGT**CTTGGTTCCACCACCGAACACAAAGTGGTTTCTGAACCATAGAGCTGCGAAGTGATTCACGTT**GCAGGTGTAG
1CH2(+)	GGACCGTCAGTCTTCCTCTTC**TTCGCAGCTCTATGGTTCAGAAACCACTTTGTGTTCGGTGGTGGAACCAAGGAGGTCACGTGC**GTGGTGGT
1CH2(−)	ACCACCACGCACGTGACCTC**CTTGGTTCCACCACCGAACACAAAGTGGTTTCTGAACCATAGAGCTGCGAAGAAGAGGAAG**ACTGACGGTCC
2CH2(+)	GAGGTCACGTGCGTGGTGGTG**TTCGCAGCTCTATGGTTCAGAAACCACTTTGTGTTCGGTGGTGGAACCAAGCAGTTCAAGTGG**TACGTGGACG
2CH2(−)	CGTCCACGTACCACTTGAACTG**CTTGGTTCCACCACCGAACACAAAGTGGTTTCTGAACCATAGAGCTGCGAACACCACCACGCA**CGTGACCTC
3CH2(+)	GGTCCAGTTCAAGTGGTACGTG**TTCGCAGCTCTATGGTTCAGAAACCACTTTGTGTTCGGTGGTGGAACCAAGAAGCCGCGGGAG**GAGCAGTAC
3CH2(−)	GTACTGCTCCTCCCGCGGCTT**CTTGGTTCCACCACCGAACACAAAGTGGTTTCTGAACCATAGAGCTGCGAACACGTACCACTTG**AACTGGACC
4CH2(+)	ACAAAGCCGCGGGAGGAGCAG**TTCGCAGCTCTATGGTTCAGAAACCACTTTGTGTTCGGTGGTGGAACCAAGTTCCGTGTGGTCA**GCGTCCTCA
4CH2(−)	TGAGGACGCTGACCACACGGAA**CTTGGTTCCACCACCGAACACAAAGTGGTTTCTGAACCATAGAGCTGCGAACTGCTCCTCCC**GCGGCTTTGT
5CH2(+)	CGTGTGGTCAGCGTCCTCACC**TTCGCAGCTCTATGGTTCAGAAACCACTTTGTGTTCGGTGGTGGAACCAAGTACAAGTGCAAG**GTCTCCAACAAAG
5CH2(−)	CTTTGTTGGAGACCTTGCACTTGTA**CTTGGTTCCACCACCGAACACAAAGTGGTTTCTGAACCATAGAGCTGCGAAGGTGAGG**ACGCTGACCACACG
6CH2(+)	GGAGTACAAGTGCAAGGTCTCC**TTCGCAGCTCTATGGTTCAGAAACCACTTTGTGTTCGGTGGTGGAACCAAGATCGAGAAAACC**ATCTCCAAAACC
6CH2(−)	GGTTTTGGAGATGGTTTTCTCGAT**CTTGGTTCCACCACCGAACACAAAGTGGTTTCTGAACCATAGAGCTGCGAAGGAGACCTT**GCACTTGTACTCC
1CH3(+)	GAACCACAGGTGTACACCCTG**TTCGCAGCTCTATGGTTCAGAAACCACTTTGTGTTCGGTGGTGGAACCAAGCAGGTCAGCCTG**ACCTGCCTG
1CH3(−)	CAGGCAGGTCAGGCTGACCTG**CTTGGTTCCACCACCGAACACAAAGTGGTTTCTGAACCATAGAGCTGCGAACAGGGTGTACAC**CTGTGGTTC
2CH3(+)	CAGCCTGACCTGCCTGGTCAAA**TTCGCAGCTCTATGGTTCAGAAACCACTTTGTGTTCGGTGGTGGAACCAAGGCCGTGGAGTGG**GAGAGCAGC
2CH3(−)	GCTGCTCTCCCACTCCACGGC**CTTGGTTCCACCACCGAACACAAAGTGGTTTCTGAACCATAGAGCTGCGAATTTGACCAGGCA**GGTCAGGCTG
3CH3(+)	CGCCGTGGAGTGGGAGAGC**TTCGCAGCTCTATGGTTCAGAAACCACTTTGTGTTCGGTGGTGGAACCAAG**TACAACACCACGCCTCCCATG
3CH3(−)	CATGGGAGGCGTGGTGTTGTA**CTTGGTTCCACCACCGAACACAAAGTGGTTTCTGAACCATAGAGCTGCGAAGCTCTCCCACTC**CACGGCG
4CH3(+)	GCCGGAGAACAACTACAACACC**TTCGCAGCTCTATGGTTCAGAAACCACTTTGTGTTCGGTGGTGGAACCAAGCTCTACAGCAAG**CTCACCGTG
4CH3(−)	CACGGTGAGCTTGCTGTAGAG**CTTGGTTCCACCACCGAACACAAAGTGGTTTCTGAACCATAGAGCTGCGAAGGTGTTGTAGTT**GTTCTCCGGC
5CH3(+)	TACAGCAAGCTCACCGTGGAC**TTCGCAGCTCTATGGTTCAGAAACCACTTTGTGTTCGGTGGTGGAACCAAGTTCTCATGCTCC**GTGATGCATGA
5CH3(−)	TCATGCATCACGGAGCATGAGAA**CTTGGTTCCACCACCGAACACAAAGTGGTTTCTGAACCATAGAGCTGCGAAGTCCACGGT**GAGCTTGCTGTA
6CH3(+)	CATCTTCTCATGCTCCGTGATG**TTCGCAGCTCTATGGTTCAGAAACCACTTTGTGTTCGGTGGTGGAACCAAGACGCAGAAGAGC**CTCTCCCTG
6CH3(−)	CAGGGAGAGGCTCTTCTGCGT**CTTGGTTCCACCACCGAACACAAAGTGGTTTCTGAACCATAGAGCTGCGAACATCACGGAGCA**TGAGAAGATG

[a] Letters in bold indicate nucleotidet encoding the (89–105)$\lambda 2^{315}$ peptide while underlining indicates nucleotide substitutions for the introduction of a silent *Dra*III site. All primers were designed with the 33 nt encoding (89–105)$\lambda 2^{315}$ in the center flanked by 18–21 nt complementary to the Cγ3wt sequence. Name according to loop of epitope grafting and domain, e.g. $1C_H1$ = epitope in loop 1 of C_H1. +/− indicates template or complementary direction, respectively.

Isolation of mutant hIgG3

Proteins in supernatants were precipitated by 1:1 addition of portions of a saturated ammonium sulfate solution. Incubation at RT for 20 min was followed by a 10-min centrifugation at 17,000 × *g* using a Sorvall centrifuge (OneMed). Pellets were dissolved in dH_2O and dialyzed three times to PBS/azide and two times to RPMI 1640 at 4°C before sterile filtration. Abs used in in vivo targeting experiments were affinity purified from cell supernatant by use of protein G-conjugated Sepharose columns.

Western blotting

Western blots were performed using Criterion XT Precast Gels (Bio-Rad). Briefly, the Ab samples were preheated at 95°C for 3 min before they were loaded onto the gel and separated at 140 V for 100 min. By Semi Dry transfer at 20 V for 30 min, proteins were transferred to an Immobilon-P polyvinylidene difluoride membrane (Sigma-Aldrich). Detection reagents were biotinylated mouse anti-hIgG3 (HP-6050) (Sigma-Aldrich) and HRP-conjugated streptavidin (GE Healthcare). Detection was performed using the ECL Plus Western Blotting Detection Reagents kit (GE Healthcare) as described by the manufacturer, and membranes were analyzed using ImageQuant TL version 2003.02 software (GE Healthcare). Individual Ab concentrations were normalized to a known concentration of purified hIgG3.

Binding to soluble FcγRIIA or protein G

The extracellular domains of hFcγRIIA were cloned and expressed as soluble fusion to GST (FcγRIIA-GST) as described elsewhere (29). ELISA plates were coated overnight at 4°C with mouse IgD at 4 μg/ml. The following day, the wells were blocked in 2% skim milk, washed three times in PBS/0.05% Tween 20, and incubated for 1 h at RT with the mutant Ab samples at 1 μg/ml. After washing, the wells were incubated for 1 h at RT with protein G-conjugated to HRP (VWR) or FcγRIIA-GST at 1 μg/ml followed by anti-GST conjugated to HRP (GE Healthcare). After three washes, the plates were developed in ABTS (Sigma-Aldrich) in citrate buffer at pH 2.2. Absorbance at 405 nm was read after 15–60 min.

In vitro Ag presentation assays

Growth inhibition assay Growth inhibition assays were performed as described by Bogen et al. (7). All Ab mutants were diluted in 5-fold series starting at 1 μg/ml and added as triplicates in flat-bottom 96-well microtiter plates. 7A10B2 T cells on day 10 after the last stimulation were irradiated (20 Gy) and 10^3 cells were added to each well along with 5000 A20δ cells in exponential growth expressing the IgD^a allotype (13). Synthetic 89–107 $\lambda 2^{315}$ peptide was included as positive control. Supernatant from cells that had had been treated with transfection reagent without DNA addition was ammonium sulfate precipitated and used as medium control. Negative control was hIgG3wt with IgD specificity. After incubation for 24 h, the cultures were pulsed with 1 μCi of [^{3}H]dThd for 16–24 h, harvested onto filters, and counted using a TopCount NXT scintillation counter (GMI).

T cell proliferation assay Samples of 5×10^5 irradiated (20 Gy) BALB/c spleen APC were cultured with 2×10^4 7A10B2 T cells and various amounts of rAb or synthetic 89–107 $\lambda 2^{315}$ peptide in triplicates for 48 h. The cultures were then pulsed with 1 μCi of [^{3}H]dThd for 16–24 h, harvested onto filters, and counted using the TopCount1 counter (GMI).

In vivo experiments

BALB/c mice were injected i.v. in the tail with titrated amounts of loop $6C_H1$ and loop $4C_H2$ rAbs. Two mice received PBS only. Ninety minutes after i.v. injections, the mice were killed by cervical dislocation and the spleens were removed. Irradiated (8 Gy) spleen cells (5×10^5/well) were cultured with responder T cells, namely, 7A10B2 or T cell hybridomas BW4B2A1 (both 2×10^4/well). An optimal concentration of the $\lambda 2^{315}$ synthetic peptide (10 μg/ml) was added to the positive control. After 72 h, portions of 100 μl of supernatant were collected for cytokine measurements, and the cultures were pulsed for 24 h with 1 μCi of [^{3}H]dThd. The cultures were harvested and incorporated [^{3}H]dThd was measured using the TopCount1 counter. Detection of IFN-γ and IL-2 in supernatants was performed in microtiter plates coated with AN18 or JES6-1A12 (both 2 μg/ml in PBS), respectively. XMG1.2-bio (1 μg/ml in PBST) was used as detection Ab for IFN-γ, whereas JES6-5H4 (1 μg/ml in PBST) was used

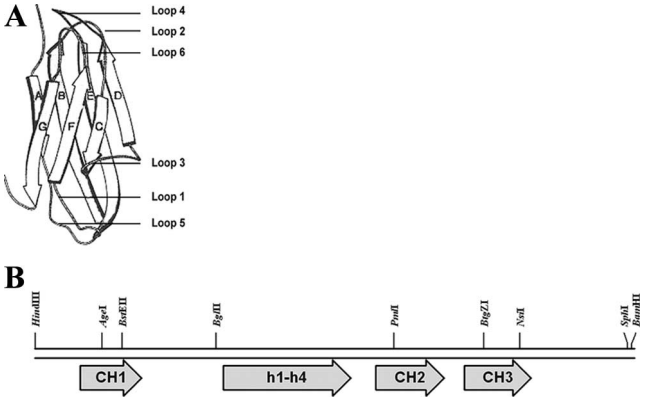

FIGURE 1. *A*, Graphic representation of a model C domain. The loops are numbered 1–6, β strands are labeled A–F. *B*, Human Cγ3 gene (ID: X03604). Exons are marked as arrows. For simplicity, the four hinge exons are shown as one exon. Restriction sites used for subcloning are indicated.

for IL-2, followed by streptavidin-alkaline phosphatase (1/3000) and 1 mg/ml *p*-nitrophenyl phosphate in diethanolamine buffer. Standard curves were prepared from a 3-fold dilution starting at 35 ng/ml IFN-γ supernatant or a 2-fold dilution starting at 2 ng/ml rIL-2 (BD Pharmingen).

Prediction of asparaginyl endopeptidase (AEP) cleavage sites

Prediction of AEP cleavage sites within every mutated hIgG3 H chain was performed with NetAEP (http://theory.bio.uu.nl/kesmir/AEP/) as provided by C. Kesmir at Utrecht University (Utrecht, The Netherlands). Distribution of every asparagine residue, from those positively identified as AEP cleavage sites to totally overlooked residues, were positioned relative to the inserted epitope and within the original secondary structure.

Prediction of MHC II peptide presentation

The presence of I-E^d binding peptides in hIgG3 H chains was predicted using the PredBALB/c server (30). Briefly, each mutant IgG3 H chain was scanned for I-E^d binding nonameric peptides. Nonamers of lower score than aa 92–100 in the $\lambda 2^{315}$ epitope (31) were excluded.

Results

Construction of mutant Cγ3 genes and secretion of recombinant Abs

Because Abs are stable molecules and may be given unique specificities that allow targeting to APC, they are ideal vehicles for delivery of amino acid sequences that contain T cell epitopes. We therefore wished to study how such a sequence of 17 aa that contains a model epitope could be introduced into a hIgG molecule. It is essential that the fusion proteins are secreted from producing cells. We focused on loop sequences that link β strands in the C_H

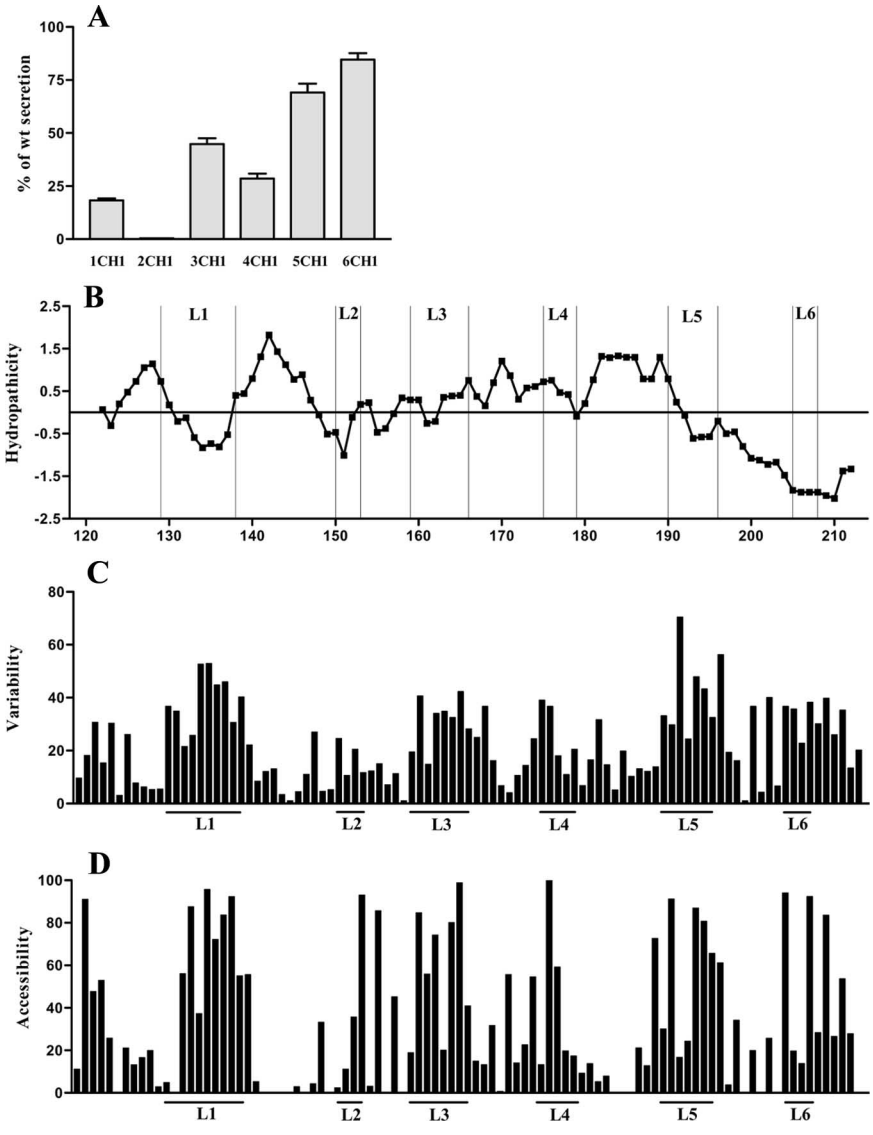

FIGURE 2. *A*, Secretion of rAb compared with wt, as determined by ELISA. Error bars indicate SD of triplicates. The graph is derived from one representative experiment of three. rAbs are named according to loop of epitope grafting and domain, i.e., $1C_H1$ = epitope in loop 1 of C_H1. *B*, Hydropathicity; *C*, Variability; and *D*, accessibility analysis of the C_H1 domain. Loop positions are indicated as L1–L6.

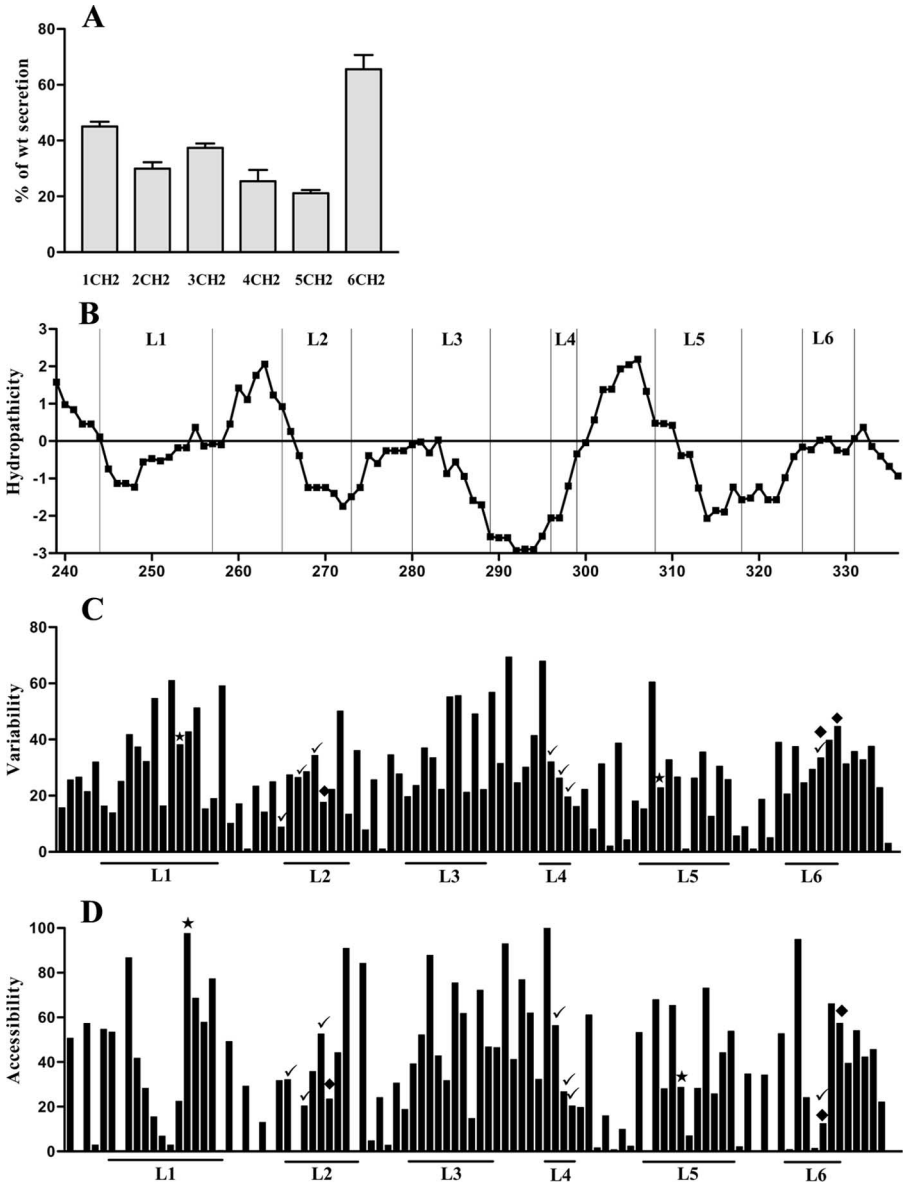

FIGURE 3. *A*, Secretion of rAb compared with wt, as determined by ELISA. Error bars indicate SD of triplicates. The graph is derived from one representative experiment of three. rAbs are named according to loop of epitope grafting and domain, i.e., $1C_H2$ = epitope in loop 1 of C_H2. *B*, Hydropathicity; *C*, variability; and *D*, accessibility analysis of the C_H2 domain. Loop positions are indicated as L1–L6. Amino acids in IgG known to be involved in effector molecule binding are indicated: ★, FcRn; √, FcγR; ♦, C1q.

domains of hIgG3. The mutant molecules should necessarily pass the endoplasmic reticulum quality control and be secreted as complete H2 plus L2 Ig (32). We did an analysis of the domain architecture and then took an empirical approach and exchanged every loop in every C_H domain with the model sequence and estimated the amounts of rAbs secreted (Figs. 2*A*, 3*A*, and 4*A*).

Since no crystal structure of a hIgG3 has been published, secondary structure analysis of individual C region domains was based on knowledge of the structure of representative IgGs, as described in *Materials and Methods*. Amino acids located in loops connecting β strands were determined and the results are presented in Table I. Although loops 1, 4, and 6 in each domain connect β strands within the same sheet, loops 2, 3, and 5 connect β strands on two opposing sheets. One-half of the 18 loops had a proline at or close to the N- or C-terminal boundary and these were defined as part of the loop rather than the framework. Hydropathicity and solvent exposure of each amino acids in all three domains were analyzed as described in *Materials and Methods*. The results are described for hydropathicity (Figs. 2*B*, 3*B*, and 4*B*) and solvent exposure (Figs. 2*C*, 3*C*, and 4*C*). We found that in C_H1, four of six loops are mostly hydrophilic while two are hydrophobic. All loops in C_H2 are either neutral or mostly hydrophilic. In C_H3, five loops are mostly hydrophilic and one is neutral in character.

The loops in the C_H2 domain have by far the largest number of amino acids that are solvent exposed, while the loops in the C_H3 domain have the largest number of buried amino acids. The majority of the loop amino acid residues with low solvent exposure point toward the domain core rather than an interdomain interface. Exceptions are single amino acid residues in loop 2 and loop $4C_H3$ that point toward the C_H3-C_H3 interface and one amino acid located in loop $2C_H1$ that point into the V region. As expected, hydrophobic regions contain many buried amino acids, mainly in frameworks, while the loops, mostly hydrophilic in nature, for the most part are exposed to the solvent.

The T cell epitope selected for study, characterized by the specificity of the T cell line 7A10B2 (7), encompasses aa 91–101 of $\lambda 2^{315}$. Notably, the aa 91–97 sequence constitutes the CDR3 loop of the V_L chain of the myeloma protein of MOPC315 (33). In this study, this sequence was extended by two amino acids N-terminally and eight amino acids C-terminally. The cysteine in position 90, which normally participates in the intradomain disulfide bond, was changed to alanine, resulting in the sequence 89-FAALW

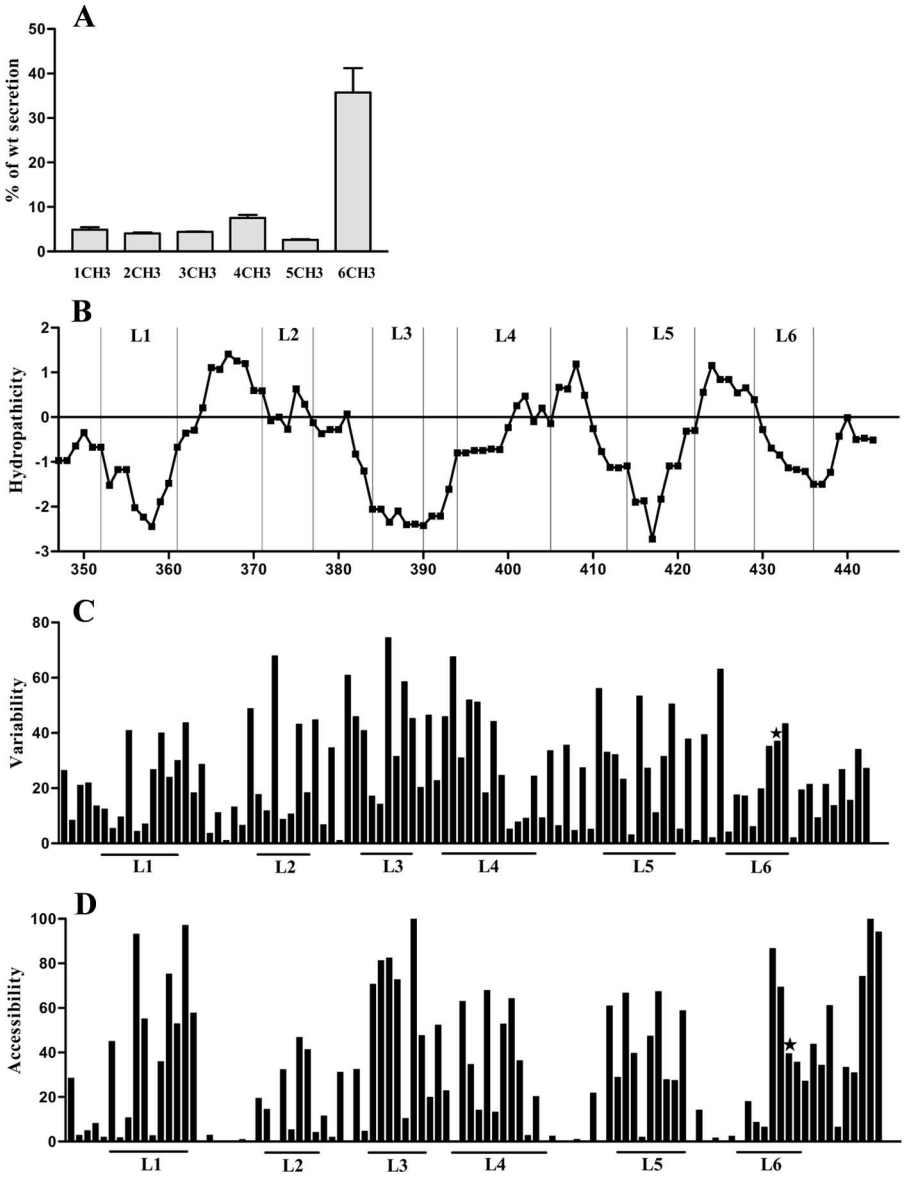

FIGURE 4. *A*, Secretion of rAb compared with wt, as determined by ELISA. Error bars indicate SD of triplicates. The graph is derived from one representative experiment of three. rAbs are named according to loop of epitope grafting and domain i.e., $1C_H3$ = epitope in loop 1 of C_H3. *B*, Hydropathicity; *C*, Variability; and *D*, accessibility analysis of C_H3. Loop positions are indicated as L1–L6. Amino acids in IgG known to be involved in effector molecule binding are indicated: ★, FcRn.

FRNHFVFGGGTK-105, and denoted 89–105 $\lambda 2^{315}$. Compared with the loop sequences that were exchanged, this is rather hydrophobic. Studies with synthetic peptides show that the Cys^{90}Ala substitution does not influence T cell responsiveness (B. Bogen, unpublished data).

We assumed that residues involved in maintaining structural stability would be rather conserved in various Ab molecules and that amino acids that were highly variable might well be substituted. We therefore performed the variability analysis for all three C_H region domains that has previously been described for C_H1 (9) (Figs. 2*D*, 3*D*, and 4*D*). In short, 144 different sequences of all isotypes from 30 species were aligned and the variability at each position was calculated as the number of different residues observed divided by the frequency of the most common residue. We found that both framework and loop sequences in all three domains contained both variable and conserved amino acids. For the most part, the loop amino acids were more variable than the framework residues. Conserved loop residues that in addition had low solvent exposure were in particular phenylalanine in loop $2C_H1$, a tryptophan residue in loop $5C_H2$ in addition to residues in all loops in C_H3.

All loops were substituted with aa 89–105 $\lambda 2^{315}$. Initially, 18 different mutants were made. Supernatants from transfectants were ammonium sulfate precipitated and dialyzed. As observed in earlier substitution experiments involving C_H1, the IgD specificity was retained in all mutants (data not shown). Secretion levels were detected by three different sandwich ELISAs using pairs of hIgG3-specific Ab. In each pair, one Ab was used as coat and the other, which was biotinylated, as detection reagent. The Abs s303, s12, and K13 used as coat had specificity for Fab, hinge, or κ L chain, respectively, whereas the detecting Abs 132c8-bio and s303-bio had specificity for hinge or Fab, respectively. The results in Figs. 2*A*, 3*A*, and 4*A* are from a representative ELISA with anti-Fab as coat and anti-hinge as detection reagent. The secretion level of wild-type (wt) IgG3 was defined as 100% and compared with the mutants. ELISAs with the two other Ab pairs gave approximately the same results. We found that all mutants were secreted at levels below wt. One mutant only, that had the mutation in loop 2 of C_H1, was completely retained. Samples of the secreted rAb run on SDS-PAGE and Western blot demonstrated that all were secreted as ~165-kDa proteins characteristic of complete H2L2 molecules (data not shown).

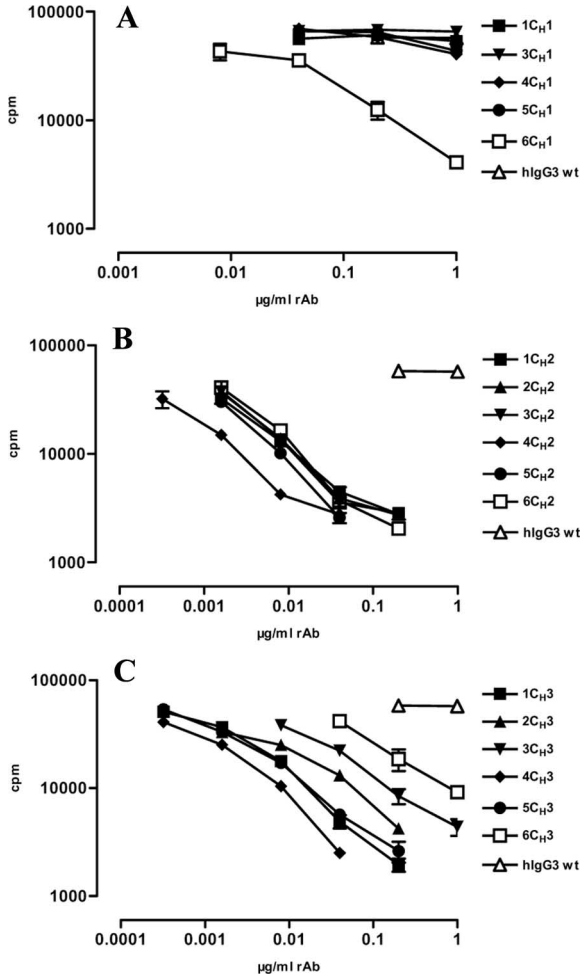

FIGURE 5. Induction of T cell activation. Mutants are compared in a growth inhibition assay. Irradiated $\lambda 2^{315}$-specific 7A10B2 $CD4^+$ T cells were cultured with A20δ B cells and IgD-specific rAbs at various concentrations. A pulse with [^{3}H]dThd was given after 16–24 h and incorporation of [^{3}H]dThd in A20δ cells was measured, reflecting growth of residual A20δ that had not been killed by activated T_H1 cells. Mutants are named as in Figs. 2–4. *A*, C_H1 mutants; *B*, C_H2 mutants; and *C*, C_H3 mutants. Error bars indicate SD of triplicates. The graphs are from one representative experiment of three.

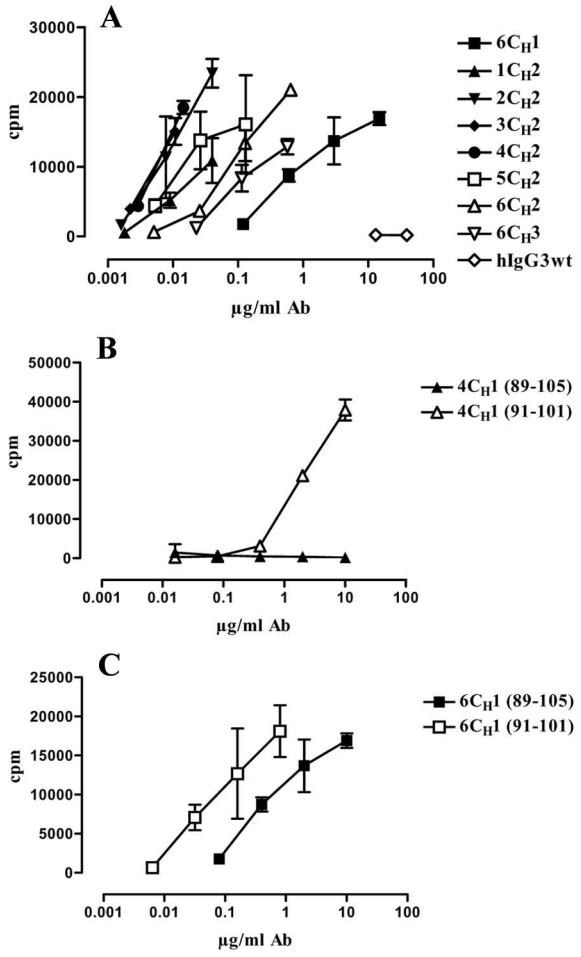

FIGURE 6. Induction of T cell activation. Mutants are compared in a T cell proliferation assay. 7A10B2 T cells were cultured with irradiated BALB/c spleen cells and rAbs at various concentrations. A pulse with [^{3}H]dThd was given after 48 h and activation was measured as incorporation of [^{3}H]dThd in T cells. *A*, IgD-specific rAb with aa 89–105 $\lambda 2^{315}$. *B* and *C*, IgD-specific rAb with long (89–105) or short (91–101) $\lambda 2^{315}$ aa sequence in loop $4C_H1$ (*B*) and loop $6C_H1$ (*C*). rAb mutants are named as in Figs. 2–4. Error bars indicate SD of triplicates. The graphs are derived from one representative experiment of two.

Comparing the secretion levels of the mutants, those with 89–105 $\lambda 2^{315}$ in loop $6C_H1$ and loop $6C_H2$ were secreted in relatively high amounts. Excluding loop $2C_H1$, all mutants with substitutions in C_H1 were secreted rather well at levels between 20 and 80% of wt. The C_H2 mutants were all secreted at 20–60% of wt, whereas for C_H3, the loop 6 mutant only was secreted in high amounts. The remaining C_H3 rAbs were secreted at levels below 10% of wt. All in all, 17 of 18 loop positions may be exchanged without complete retention and 12 without more than a 5-fold reduction in secretion.

Activation of specific T cells

It is crucial that the mutants are internalized by APC so as to enter the Ag-processing pathway and that the specific epitopes are properly excised from the rAb carrier to bind MHC and transported as peptide-MHC complexes to the cell surface. In this study, the mutant hIgG3s were tested in two different in vitro T cell activation assays, namely, a growth inhibition assay and a T cell proliferation assay.

Growth inhibition assay

The T_H 1 cell clone used (7A10B2) has cytotoxic activity toward A20 lymphoma APC upon ligand recognition (7). The assay readout, incorporated radioactivity, reflects growth of the lymphoma cell APC only, as the T cells are irradiated. The assay is at least 10-fold more sensitive than a conventional T cell proliferation assay. The APC had been transfected with genes encoding IgD^a (13) and were thus targets for the IgD-specific mutants. Irradiated 7A10B2 Th1 cells were mixed with secreted rAb mutants and APC as described in *Materials and Methods* (Fig. 5).

We found that the APC mixed with all rAb-harboring epitopes in C_H2 or C_H3 loops activated specific T cells, with C_H2 replacements being more effective and with less variation than C_H3 replacements. Thus, the epitope was presented to T cells from all positions in C_H2 and C_H3. However, from C_H1, the epitope was detectably presented from loop 6 only. Notably, a high amount of loop $6C_H1$ was needed to obtain the effect. At 0.01 μg/ml, a concentration that was sufficient to induce the effect of all C_H2 and C_H3 mutants, no growth inhibition was detected. Thus, the epitopes in loops of C_H1 seemed to be somewhat protected from presentation.

T cell proliferation assay

To confirm the results from the growth inhibition assay, eight mutants were selected, namely, loop $6C_H1$, all C_H2 mutants, and loop

Table III. *List of hIgG3 mutants*

Domain	Loop	Loop Sequence[a]	Amino Acid Length Difference[b]	Secretion[c]	Activation[d]
C_H1	1	APC^{1}SRSTSGG	7	++	−
	2	F^{2}P^{2}EP	13	−	ND
	3	NSGALTSG	9	++	−
	4	QSSGL	12	++	−
	5	PSSSLGTQ	8	++	−
	6	KPSN	13	+++	+
C_H2	1	PPKPKDTLMI^{3}SRTP	3	++	++
	2	D^{4}VS^{4}HE^{4}D^{5}PEV	8	++	+++
	3	DGVEVHNAKT	7	++	+++
	4	YN^{4}S^{4}T^4	8	++	+++
	5	VLH^{3}QDWLNGKE	6	++	++
	6	NKALP^{4,5}AP^5	10	+++	++
C_H3	1	PPSREEMTKN	7	+	++
	2	GFYPSDI	10	+	++
	3	SGQPENN	10	+	+
	4	TPPMLDSDGSFF	5	+	++
	5	KSRWQQGNI	8	+	++
	6	HEALHNR^{3}F	9	++	+

[a] Underlining indicates that an amino acid is displaying <10% variation. Superscript numbers indicate that an amino acid is involved in binding an effector molecule or has an important structural feature. 1, H-L chain pairing (34); 2, ball and socket joint (35); 3, FcRn binding (36); 4: FcγR binding (37); 5, C1q binding (38).

[b] Indicates loop length differences after replacement of the native loop with the (89–105) $\lambda2^{315}$ epitope.

[c] Secretion levels: +++ indicates secretion at 50–100%, ++ indicates secretion at 10–49%, and + indicates secretion at 1–9% of wild-type level.

[d] T cell activation induced by the corresponding mutant.

$6C_H3$, all of which were secreted at levels above 20% of wt. These were further tested in a T cell proliferation assay. BALB/c spleen cells as APC, T cells, and rAbs were combined. The APC were irradiated and, thus, in this case, incorporation of radioactivity reflects T cell proliferation upon Ag stimulation. All mutants tested induced proliferation of the specific T cells (Fig. 6*A*). As in the growth inhibition assays, the mutants with epitopes in either of loops 2, 3, or $4C_H2$ were the most efficient T cell activators, followed by those with epitope in loops 1, 5, or 6 C_H2, which showed intermediate activation ability. Both loop $6C_H1$ and loop $6C_H3$ mutants required ~100× higher concentration than the best mutants to induce proper activation. A hierarchy appeared where loop $2C_H2 = 3C_H2 = 4C_H2 > 5C_H2 > 1C_H2 > 6C_H2 > 6\ C_H3 > 6C_H1$. The results correspond well to those obtained in the APC growth inhibition assay. A summary of results from the secretion and T cell activation assays are presented in Table III.

A loop $4C_H1$ mutant has previously proved to induce T cell activation (8). This mutant was identical to the one tested here, except for the fact that a short sequence of 11 aa, namely, 91–101 $\lambda2^{315}$, was introduced. To test whether the 89–105 sequence of 17 aa was less efficient than 91–101, two mutants with the long and two mutants with the short sequence in loop 4 or 6 of C_H1, respectively, were compared side-by-side in the T cell proliferation assay. In each case, the mutant with short sequence was indeed found to be more efficient than the corresponding mutant with a long sequence (Fig. 6, *B* and *C*).

T cell activation after in vivo targeting

One of the most active C_H2 mutants, namely, loop $4C_H2$, was selected for further characterization in vivo and compared side-by-side with the loop $6C_H1$ mutant. Both were injected in BALB/c mice at various concentrations, and after 90 min the spleens were removed and whole spleen cell preparations mixed with specific T cells in vitro. T cell activation was measured as proliferation, IFN-γ secretion or IL-2 secretion, as a function of dose injected. Thus, in vivo APC targeting and processability of the two rAbs was compared in normal mice that express the relevant MHC class II molecule as previously described (11). Two different T cell preparations were used, 7A10B2 as described above and a T cell hybridoma derived from a mouse transgenic for the TCR of the T cell line 4B2A1. 7A10B2 and 4B2A1 have the same specificity (7). The dose-response curves are shown in Fig. 7. In all cases, whether measuring proliferation (Fig. 7*A*), IFN-γ production (Fig. 7*B*), or IL-2 production (Fig. 7*C*), the loop $4C_H2$ mutant induced specific T cell activation at concentrations at least 10^2-fold lower than loop $6C_H1$, and detectable activation was found after injection of ~1 μg of loop $4C_H2$ rAb per mouse.

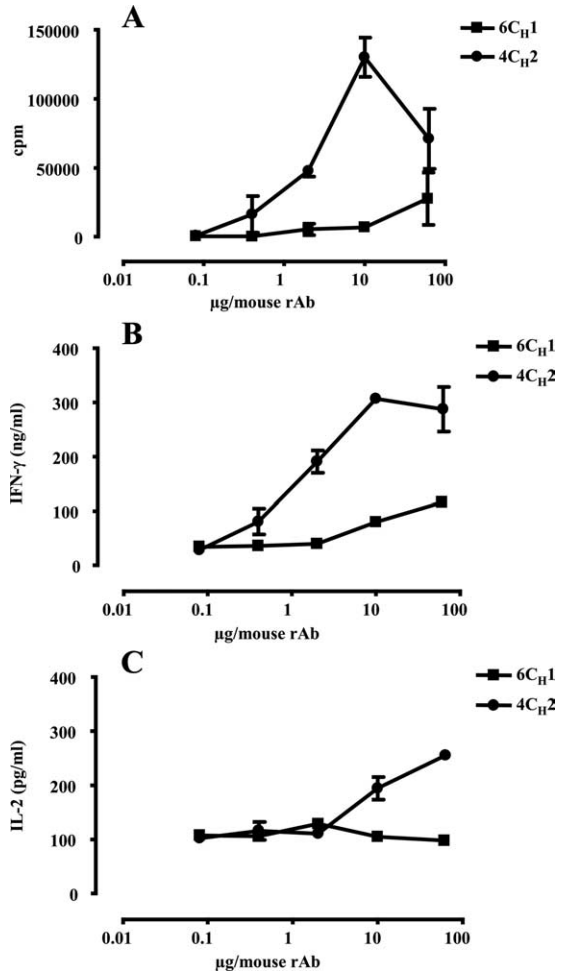

FIGURE 7. Induction of T cell activation after rAb injection in BALB/c mice and in vivo targeting. Titrated amounts of loop $4C_H2$ and loop $6C_H1$ rAbs were injected i.v. (two mice per point). After 90 min, the spleens were removed and the splenocytes were irradiated and used as APC in coculture with specific T cells: 7A10B2 for 72 h (*A* and *B*) or BW4B2A1 T cell hybridomas for 48 h (*C*). *A*, The cells were pulsed with [^{3}H]dThd and T cell proliferation was measured as incorporation of radioactivity. *B*, IFN-γ produced was measured by ELISA. *C*, IL-2 produced was measured by ELISA. Error bars indicate SD of triplicates.

Binding studies

The eight rAbs were tested for binding to FcγRIIA and protein G. In general, IgGs bind ligands in either of two Fc locations, namely, the lower hinge (all FcγR as well as C1q) or the elbow region between C_H2 and C_H3 (protein A, protein G, FcRn) (39). To investigate the integrity of these two regions in the mutants, they were tested in ELISA for binding to recombinant soluble FcγRIIA and protein G, respectively. Mouse IgD was coated in the wells followed by the various IgD-specific rAbs. As was to be expected, the loop $6C_H1$ mutant bound both protein G and FcγRIIA (Fig. 8, *A* and *B*). Although none of the other seven mutants bound FcγRIIA, the loop

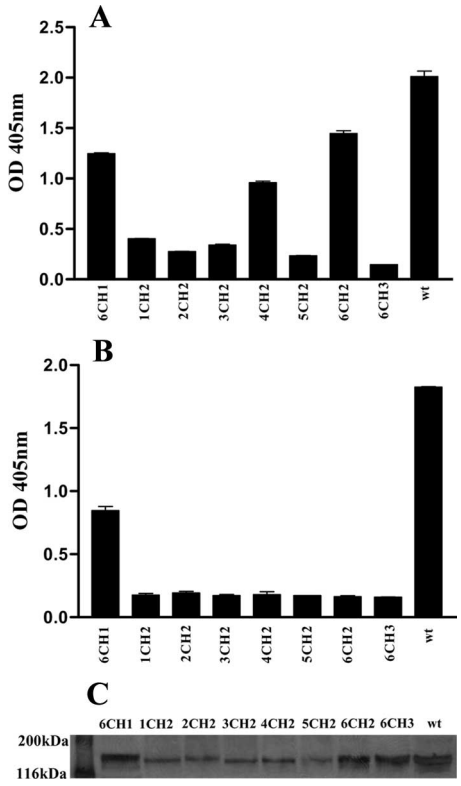

FIGURE 8. Ab binding protein G and soluble FcγRIIA in ELISA. *A* and *B*, Mouse IgD was coat and IgD-specific rAb were added as well as protein G (*A*) and soluble recombinant FcγRIIA (*B*). Error bars indicate SD of triplicates. The graphs are derived from one representative experiment of two. *C*, Western blot detection of each rAb preparation with a hIgG3 hinge-specific Ab. Mutants are named as in Figs. 2–4.

$4C_H2$ and loop $6C_H2$ mutants bound protein G. The relative amount of rAb that was added to each well was visualized by Western blotting, detected with a hIgG3 hinge- specific Ab (Fig. 8*C*).

Discussion

We expected that substitution of constant region loops with a different amino acid sequence would influence the stability and, therefore, secretion, of the fusion molecules. In general, amino acids that are important for thermodynamic stability can be involved in packing of the hydrophobic core, charge interactions, hydrogen bonding, desolvation upon folding, and be more or less compatible with the enforced local structure (40). Regarding C_H1, this domain interacts with C_L through a large, well-packed hydrophobic interface that enhances the stability of both domains (34). Furthermore, the variability and surface accessibility of loop amino acids in the C_H1 domain is notable. Therefore, it was not surprising that the mutants with substitution of loops in this domain were well secreted. An exception is the loop $2C_H1$ mutant that was completely retained. This is in agreement with previous results (9) and confirms that removal of the ball-and-socket joint (35) between V_H and C_H1 that involves this loop, is detrimental to secretion of hIgG3. A corresponding mutant in mIgG2b is secreted, however (9), and, therefore, the requirement for the interaction is not absolute. The amino acids involved in the C_H1/C_L interface are mostly situated in the A, B, D, and E strands, separated by loops 1 and 4, respectively. Substitution of these loops was less well tolerated than substitution of loops 3 and 6.

The C_H2 domains do not physically interact with each other, they are heavily glycosylated on the Asn^{297} residue situated in loop 4, and the carbohydrate moiety normally fills the space between the domains. Mutating loop 4 decreased the secretion level 4-fold. However, all C_H2 loop mutants were secreted in amounts between 20 and 60% of wt level, and the reduction may therefore not easily be attributed to removal of the carbohydrate. Of the C_H2 loop mutants, that in loop 5 showed the lowest secretion, probably due to removal of the conserved and buried tryptophan in the native loop sequence.

The C_H3 domain contains several amino acids that contribute to either the interface between C_H2 and C_H3 or dimerization through C_H3-C_H3 domain interaction and consequently have low accessibility scores. Variability analysis demonstrated the presence of many conserved residues in this domain, both in frameworks and in loops. The C_H3-C_H3 interface involves 16 residues that make interchain contacts (41). Of these, dimer stabilization is largely mediated by two loop 4 residues and four β strand residues. Thus, substitution of the involved loop $4C_H3$ may have destabilized the domain interface, whereas the other loop mutations may well have altered the configuration of β strands to reduce overall domain stability. It is therefore not surprising that the secretion of all but one mutant, namely, that involving loop 6, was very low. In this study, the new sequence is introduced at the outer edge of the domain and destabilizing effects introduced may have left the domain core mostly unaffected. The introduced 17 aa increased the loop length of all mutants from 3 to 13 aa. Those secreted in high amounts were all elongated from 10 to 13 aa (Table III). In a previous study, loop $6C_H1$ was exchanged with epitopes as long as 37 aa without interrupting secretion (42). Thus, long sequences may be introduced.

Proline residues at the framework/loop boundaries were defined as part of the loop by the Swiss-Pdb Viewer program and removed upon introduction of the 89–105 $\lambda 2^{315}$ sequence. In one case, the loop $5C_H1$ mutant was made both with and without an N-terminal proline and the presence of proline improved secretion 4-fold (M. Flobakk, unpublished data). Thus, secretion may be further improved by keeping or possibly adding prolines to the framework/loop boundaries.

As we addressed ligand binding, we observed that the mutant with the new sequence in Fab bound both FcγRIIA and protein G. None of the mutants with insert in the Fc region bound FcγRIIA, whereas two bound protein G, namely, the loop $4C_H2$ and the loop $6C_H1$ mutants. A lack of FcγR binding may be an advantage, as the function of IgG in the context of the studies reported here, is solely to target APC by way of V region specificity. Protein G binds in a region remote from the FcγR binding site, namely, at the interface of C_H2 and C_H3 which is also the site of FcRn binding, and alterations here are likely to affect biodistribution and half-life of the mutant in vivo (36).

Specific growth inhibition and T cell proliferation assays were used to monitor peptide presentation on MHC class II and thus processing and loading of all mutants in vitro. The epitope was excised and presented to T cells from 13 of 18 positions in the rAb, and there were variations in activation efficiency. The mutants with substitution in loops of C_H1 did not induce T cell activation, with the exception of loop $6C_H1$, which did so with a relatively low activity. All of the C_H2 mutants induced with a high activity and, in particular, the mutant with epitope in loop 4, which was the better inducer in both the growth inhibition and T cell proliferation experiment. To induce the same in vitro effect, 100× less rAb of the loop $4C_H2$ than the loop $6C_H1$ variant was needed. The mutants with epitope in either of the C_H3 domain loops activated at various levels. Of these, the loop $6C_H3$ mutant, which unlike the other C_H3 mutants, was secreted well, had low in vitro activity, almost as low as loop $6C_H1$.

The C_H1 domain seemed to be somewhat resistant to intracellular processing. This was not an effect of the epitope chosen, as the same result was obtained for the unrelated sequence of the

OVA epitope, aa 323–339. Although an $OVA_{323–339}$ loop $6C_H1$ mutant induced activation (10), an $OVA_{323–326}$ loop $1C_H1$ mutant did not (M. Flobakk, unpublished data). Furthermore, we have previously observed very poor presentation of the $\lambda2^{315}$ sequence from loop 2 and $4C_H1$ in mIgG2, and the observation is therefore not restricted to hIgG3 (9) (Note that mutant terminology differs in this article.) In all cases were the C_H2 domain mutants well secreted from producing cells and induced T cell activation at low concentrations. Again, the finding was not restricted to the amino acid sequence chosen for the systematic substitution experiments, as analogous fusion molecules with aa 110–120 from the hemagglutinin epitope in loop $1C_H2$ or aa 46–61 from the hen egg lysozyme in loop $6C_H2$ were well secreted and induced T cell activation in vitro at the same low rAb concentrations (M. Flobakk, I. B. Rasmussen, E. Lunde, T. E., Michaelsen, B. Bogen, and I. Sandlie, submitted for publication). In conclusion, a total of eight loop mutants were found to be useful for T cell activation purposes when both secretion from producing cells and the ability to induce activation in vitro were considered.

Of these, two were chosen for in vivo investigation, namely, loop $6C_H1$ and loop $4C_H2$. One harbors the epitope in Fab and one in Fc and they have a remarkable 100-fold difference in T cell activation efficiency in vitro. Importantly, this difference was also seen in vivo. Others have demonstrated that stability is inversely related to processing and. thus, to presentation in vitro. In vivo, the situation was reversed and the stable molecule induced a stronger T cell response than the unstable variant (43, 44). In the experiment presented here, on the other hand, the mutants were actively targeted to APC in vivo. Because we have previously shown that presentation peaks when the targeted spleen cells are removed and tested for T cell activation ability after 1–2 h (11), it is reasonable to believe that both mutants are stable in serum until internalized.

We were intrigued by the fact that the C_H1 domain mutants were poor inducers of T cell activation and speculated that there might not be recognition sites for proteolytic enzymes adjacent to the epitope in the C_H1 domain. Although most proteases have broad specificity, making processing predictions difficult, AEP has restricted specificity (45). It cleaves at selected asparagine residues and unlocks the globular protein structure for MHC class II screening (46). There are 14 asparagine residues in the $C_\gamma3$ amino acid sequence (26), and the AEP cleavage server (http://theory.bio.uu.nl/keshmir/AEP) predicts five cleavage sites in the Fc region and only one in C_H1. Thus, additional recognition sites in C_H1 might improve the activation potential of the C_H1 mutants. Notably, the 89–105 $\lambda2^{315}$ sequence also contains an asparagine residue (Asn^{96}), but according to the AEP cleavage server, it is not susceptible to AEP cleavage regardless of its position within any C_H domain.

Peptides presented on $I\text{-}E^d$ are anchored at positions P1, P4, P6, and P9 (31). The anchor residues in 89–105 $\lambda2^{315}$ are Leu^{92}, Phe^{94}, Arg^{95}, and Phe^{100} within the epitope (91–101). Competing $I\text{-}E^d$ binding motifs could disturb 91–101 epitope loading. The $Pred^{BALB/c}$ server (http://Ag.i2r.a-star.edu.sg/predBALBc/) predicts nonamer peptide binding to the $H\text{-}2^d$ haplotype of BALB/c mice (30). Focusing on nonamers with an equal to or higher score than 92–100, 25 peptides in Cγ3wt were identified that may compete for $I\text{-}E^d$ binding, but there does not seem to be an obvious correlation between the location of these peptides and activation efficiency. Importantly, the 89–105 sequence was found to encompass an additional nonamer, namely, 97–105 (HFVFGGGTK) that fits better in $I\text{-}E^d$ than 92–100. These two are mutually exclusive and this may explain the finding that the long peptide of 17 aa induced activation of aa 91–101-specific T cells at a lower level than the short peptide of only 11 aa in two different mutants (loop $4C_H1$ and loop $6C_H1$).

In the experiments shown here, APC were targeted by anti-mouse IgD^a, i.e., to the Ag receptor of B cells (13). This is an endocytic receptor that directs Troybodies to intracellular vesicles where Ag processing and epitope loading on MHC class II occur. However, the B cell receptors are not optimal targets in vivo and a major disadvantage is the possibility for polyclonal activation of B cells (47). Alternative targets are surface molecules such as CD19 on B cells (48), MHC class II (48, 49), and CD14 (50). Receptors on dendritic cells may be even better targets since dendritic cells are able to prime naive T cells and induce T_H, $T_{C,}$ and B cell responses. CD40 (51, 52), TLR (53, 54), CD91 (55), several chemokine receptors (56, 57), and C-type lectins, such as DC-SIGN (58, 59), mannose receptor (60), and DEC-205 (61, 62), have all been shown to be attractive candidates for targeting.

Our results are clear regarding an activation hierarchy in vitro and in vivo. rAbs with epitope loaded in the C_H2 domain are secreted from producing cells and processed very efficiently after targeting to APC. Thus, whenever the goal is strong enhancement of T cell responses, epitope grafting in the C_H2 domain seems preferable. For vaccination purposes, integration of several different sequences may be desirable. The results presented here suggest that multiple loop replacements within a single rAb may be a useful strategy using a combination of loop substitutions in two or possibly three domains.

Acknowledgments

We are grateful to Hilde Omholt, Peter Hofgaard, and Karoline W. Schjetne for help during the T cell assays and Kristine Ustgård for FcγRIIA.

Disclosures

Inger Sandlie and Bjarne Bogen are coinventors on U.S. patent 6.249.654 granted September 25, 2001. Title: Modified immunoglobulin molecule incorporating antigen in a non-CDR loop region.

References

1. Snider, D. P., and D. M. Segal. 1987. Targeted antigen presentation using cross-linked antibody heteroaggregates. *J. Immunol.* 139: 1609–1616.
2. Bona, C. A., S. Casares, and T. D. Brumeanu. 1998. Towards development of T-cell vaccines. *Immunol. Today* 19: 126–133.
3. Baier, G., G. Baier-Bitterlich, D. J. Looney, and A. Altman. 1995. Immunogenic targeting of recombinant peptide vaccines to human antigen- presenting cells by chimeric anti-HLA-DR and anti-surface immunoglobulin D antibody Fab fragments in vitro. *J. Virol.* 69: 2357–2365.
4. Hawiger, D., K. Inaba, Y. Dorsett, M. Guo, K. Mahnke, M. Rivera, J. V. Ravetch, R. M. Steinman, and M. C. Nussenzweig. 2001. Dendritic cells induce peripheral T cell unresponsiveness under steady state conditions in vivo. *J. Exp. Med.* 194: 769–779.
5. Trumpfheller, C., J. S. Finke, C. B. Lopez, T. M. Moran, B. Moltedo, H. Soares, Y. Huang, S. J. Schlesinger, C. G. Park, M. C. Nussenzweig, et al. 2006. Intensified and protective $CD4^+$ T cell immunity in mice with anti-dendritic cell HIV gag fusion antibody vaccine. *J. Exp. Med.* 203: 607–617.
6. Bogen, B., and J. D. Lambris. 1989. Minimum length of an idiotypic peptide and a model for its binding to a major histocompatibility complex class II molecule. *EMBO J.* 8: 1947–1952.
7. Bogen, B., B. Malissen, and W. Haas. 1986. Idiotope-specific T cell clones that recognize syngeneic immunoglobulin fragments in the context of class II molecules. *Eur. J. Immunol.* 16: 1373–1378.
8. Lunde, E., B. Bogen, and I. Sandlie. 1997. Immunoglobulin as a vehicle for foreign antigenic peptides immunogenic to T cells. *Mol. Immunol.* 34: 1167–1176.
9. Eidem, J. K., I. B. Rasmussen, E. Lunde, T. F. Gregers, A. R. Rees, B. Bogen, and I. Sandlie. 2000. Recombinant antibodies as carrier proteins for sub-unit vaccines: influence of mode of fusion on protein production and T-cell activation. *J. Immunol. Methods* 245: 119–131.
10. Rasmussen, I. B., E. Lunde, T. E. Michaelsen, B. Bogen, and I. Sandlie. 2001. The principle of delivery of T cell epitopes to antigen-presenting cells applied to peptides from influenza virus, ovalbumin, and hen egg lysozyme: implications for peptide vaccination. *Proc. Natl. Acad. Sci. USA* 98: 10296–10301.
11. Lunde, E., L. A. Munthe, A. Vabo, I. Sandlie, and B. Bogen. 1999. Antibodies engineered with IgD specificity efficiently deliver integrated T-cell epitopes for antigen presentation by B cells. *Nat. Biotechnol.* 17: 670–675.
12. Lunde, E., K. H. Western, I. B. Rasmussen, I. Sandlie, and B. Bogen. 2002. Efficient delivery of T cell epitopes to APC by use of MHC class II-specific Troy bodies. *J. Immunol.* 168: 2154–2162.

13. Tisch, R., M. Watanabe, M. Letarte, and N. Hozumi. 1987. Assessment of antigen-specific receptor function of surface immunoglobulin M and D with identical hapten specificity. *Proc. Natl. Acad. Sci. USA* 84: 3831–3835.
14. Bogen, B., L. Gleditsch, S. Weiss, and Z. Dembic. 1992. Weak positive selection of transgenic T cell receptor-bearing thymocytes: importance of major histocompatibility complex class II, T cell receptor and CD4 surface molecule densities. *Eur. J. Immunol.* 22: 703–709.
15. White, J., M. Blackman, J. Bill, J. Kappler, P. Marrack, D. P. Gold, and W. Born. 1989. Two better cell lines for making hybridomas expressing specific T cell receptors. *J. Immunol.* 143: 1822–1825.
16. Prat, M., G. Gribaudo, P. M. Comoglio, G. Cavallo, and S. Landolfo. 1984. Monoclonal antibodies against murine γ interferon. *Proc. Natl. Acad. Sci. USA* 81: 4515–4519.
17. Cherwinski, H. M., J. H. Schumacher, K. D. Brown, and T. R. Mosmann. 1987. Two types of mouse helper T cell clone. III. Further differences in lymphokine synthesis between Th1 and Th2 clones revealed by RNA hybridization, functionally monospecific bioassays, and monoclonal antibodies. *J. Exp. Med.* 166: 1229–1244.
18. Fjeld, J. G., T. E. Michaelsen, and K. Nustad. 1992. The binding parameters of radiolabelled monoclonal $F(ab')_2$ and Fab′ fragments relative to immunoglobulin G in reactions with surface-bound antigens. *Eur. J. Nucl. Med.* 19: 402–408.
19. Jefferis, R., C. B. Reimer, F. Skvaril, G. de Lange, N. R. Ling, J. Lowe, M. R. Walker, D. J. Phillips, C. H. Aloisio, T. W. Wells, et al. 1985. Evaluation of monoclonal antibodies having specificity for human IgG sub-classes: results of an IUIS/WHO collaborative study. *Immunol. Lett.* 10: 223–252.
20. Aaberge, I. S., T. E. Michaelsen, A. K. Rolstad, E. C. Groeng, P. Solberg, and M. Lovik. 1992. SCID-Hu mice immunized with a pneumococcal vaccine produce specific human antibodies and show increased resistance to infection. *Infect. Immun.* 60: 4146–4153.
21. Michaelsen, T. E., A. Aase, C. Westby, and I. Sandlie. 1990. Enhancement of complement activation and cytolysis of human IgG3 by deletion of hinge exons. *Scand. J. Immunol.* 32: 517–528.
22. Berman, H. M., J. Westbrook, Z. Feng, G. Gilliland, T. N. Bhat, H. Weissig, I. N. Shindyalov, and P. E. Bourne. 2000. The Protein Data Bank. *Nucleic Acids Res.* 28: 235–242.
23. Saphire, E. O., R. L. Stanfield, M. D. Crispin, G. Morris, M. B. Zwick, R. A. Pantophlet, P. W. Parren, P. M. Rudd, R. A. Dwek, D. R. Burton, and I. A. Wilson. 2003. Crystal structure of an intact human IgG: antibody asymmetry, flexibility, and a guide for HIV-1 vaccine design. *Adv. Exp. Med. Biol.* 535: 55–66.
24. Gasteiger, E., C. Hoogland, A. Gattiker, S. Duvaud, M. R. Wilkins, R. D. Appel, and A. Bairoch. 2005. Protein identification and analysis tools on the ExPASy. In *The Proteomics Protocols Handbook.* John M. Walker, ed. Humana Press, Totowa, NJ, pp. 571–607.
25. Kyte, J., and R. F. Doolittle. 1982. A simple method for displaying the hydropathic character of a protein. *J. Mol. Biol.* 157: 105–132.
26. Huck, S., P. Fort, D. H. Crawford, M. P. Lefranc, and G. Lefranc. 1986. Sequence of a human immunoglobulin γ 3 heavy chain constant region gene: comparison with the other human C γ genes. *Nucleic Acids Res.* 14: 1779–1789.
27. Norderhaug, L., T. Olafsen, T. E. Michaelsen, and I. Sandlie. 1997. Versatile vectors for transient and stable expression of recombinant antibody molecules in mammalian cells. *J. Immunol. Methods* 204: 77–87.
28. Berntzen, G., E. Lunde, M. Flobakk, J. T. Andersen, V. Lauvrak, and I. Sandlie. 2005. Prolonged and increased expression of soluble Fc receptors, IgG and a TCR-Ig fusion protein by transiently transfected adherent 293E cells. *J. Immunol. Methods* 298: 93–104.
29. Berntzen, G., O. H. Brekke, S. A. Mousavi, J. T. Andersen, T. E. Michaelsen, T. Berg, I. Sandlie, and V. Lauvrak. 2006. Characterization of an FcγRI-binding peptide selected by phage display. *Protein Eng. Des. Sel.* 19: 121–128.
30. Zhang, G. L., K. N. Srinivasan, A. Veeramani, J. T. August, and V. Brusic. 2005. PREDBALB/c: a system for the prediction of peptide binding to $H2^d$ molecules, a haplotype of the BALB/c mouse. *Nucleic Acids Res.* 33: W180–W183.
31. Schild, H., U. Gruneberg, G. Pougialis, H. J. Wallny, W. Keilholz, S. Stevanovic, and H. G. Rammensee. 1995. Natural ligand motifs of H-2E molecules are allele specific and illustrate homology to HLA-DR molecules. *Int. Immunol.* 7: 1957–1965.
32. Ellgaard, L., and A. Helenius. 2003. Quality control in the endoplasmic reticulum. *Nat. Rev. Mol. Cell Biol.* 4: 181–191.
33. Bothwell, A. L., M. Paskind, M. Reth, T. Imanishi-Kari, K. Rajewsky, and D. Baltimore. 1982. Somatic variants of murine immunoglobulin λ light chains. *Nature* 298: 380–382.
34. Rothlisberger, D., A. Honegger, and A. Pluckthun. 2005. Domain interactions in the Fab fragment: a comparative evaluation of the single-chain Fv and Fab format engineered with variable domains of different stability. *J. Mol. Biol.* 347: 773–789.
35. Lesk, A. M., and C. Chothia. 1988. Elbow motion in the immunoglobulins involves a molecular ball-and-socket joint. *Nature* 335: 188–190.
36. Kim, J. K., M. Firan, C. G. Radu, C. H. Kim, V. Ghetie, and E. S. Ward. 1999. Mapping the site on human IgG for binding of the MHC class I-related receptor, FcRn. *Eur. J. Immunol.* 29: 2819–2825.
37. Sondermann, P., R. Huber, V. Oosthuizen, and U. Jacob. 2000. The 3.2-Å crystal structure of the human IgG1 Fc fragment-Fc γRIII complex. *Nature* 406: 267–273.
38. Idusogie, E. E., L. G. Presta, H. Gazzano-Santoro, K. Totpal, P. Y. Wong, M. Ultsch, Y. G. Meng, and M. G. Mulkerrin. 2000. Mapping of the C1q binding site on rituxan, a chimeric antibody with a human IgG1 Fc. *J. Immunol.* 164: 4178–4184.
39. Nezlin, R., and V. Ghetie. 2004. Interactions of immunoglobulins outside the antigen-combining site. *Adv. Immunol.* 82: 155–215.
40. Ewert, S., A. Honegger, and A. Pluckthun. 2003. Structure-based improvement of the biophysical properties of immunoglobulin VH domains with a generalizable approach. *Biochemistry* 42: 1517–1528.
41. Dall'Acqua, W., A. L. Simon, M. G. Mulkerrin, and P. Carter. 1998. Contribution of domain interface residues to the stability of antibody CH3 domain homodimers. *Biochemistry* 37: 9266–9273.
42. Tunheim, G., K. W. Schjetne, I. B. Rasmussen, L. M. Sollid, I. Sandlie, and B. Bogen. 2008. Recombinant antibodies for delivery of antigen: a single loop between β-strands in the constant region can accommodate long, complex and tandem T cell epitopes. *Int. Immunol.* 20: 295–306.
43. Thai, R., G. Moine, M. Desmadril, D. Servent, J. L. Tarride, A. Menez, and M. Leonetti. 2004. Antigen stability controls antigen presentation. *J. Biol. Chem.* 279: 50257–50266.
44. So, T., H. O. Ito, T. Koga, S. Watanabe, T. Ueda, and T. Imoto. 1997. Depression of T-cell epitope generation by stabilizing hen lysozyme. *J. Biol. Chem.* 272: 32136–32140.
45. Chen, J. M., P. M. Dando, N. D. Rawlings, M. A. Brown, N. E. Young, R. A. Stevens, E. Hewitt, C. Watts, and A. J. Barrett. 1997. Cloning, isolation, and characterization of mammalian legumain, an asparaginyl endopeptidase. *J. Biol. Chem.* 272: 8090–8098.
46. Manoury, B., E. W. Hewitt, N. Morrice, P. M. Dando, A. J. Barrett, and C. Watts. 1998. An asparaginyl endopeptidase processes a microbial antigen for class II MHC presentation. *Nature* 396: 695–699.
47. Finkelman, F. D., I. Scher, J. J. Mond, S. Kessler, J. T. Kung, and E. S. Metcalf. 1982. Polyclonal activation of the murine immune system by an antibody to IgD: II. Generation of polyclonal antibody production and cells with surface IgG. *J. Immunol.* 129: 638–646.
48. Yan, J., M. J. Wolff, J. Unternaehrer, I. Mellman, and M. J. Mamula. 2005. Targeting antigen to CD19 on B cells efficiently activates T cells. *Int. Immunol.* 17: 869–877.
49. Casten, L. A., and S. K. Pierce. 1988. Receptor-mediated B cell antigen processing: increased antigenicity of a globular protein covalently coupled to antibodies specific for B cell surface structures. *J. Immunol.* 140: 404–410.
50. Tunheim, G., K. W. Schjetne, A. B. Fredriksen, I. Sandlie, and B. Bogen. 2005. Human CD14 is an efficient target for recombinant immunoglobulin vaccine constructs that deliver T cell epitopes. *J. Leukocyte Biol.* 77: 303–310.
51. Tillman, B. W., T. D. de Gruijl, S. A. Luykx-de Bakker, R. J. Scheper, H. M. Pinedo, T. J. Curiel, W. R. Gerritsen, and D. T. Curiel. 1999. Maturation of dendritic cells accompanies high-efficiency gene transfer by a CD40-targeted adenoviral vector. *J. Immunol.* 162: 6378–6383.
52. Schjetne, K. W., A. B. Fredriksen, and B. Bogen. 2007. Delivery of antigen to CD40 induces protective immune responses against tumors. *J. Immunol.* 178: 4169–4176.
53. Schjetne, K. W., K. M. Thompson, N. Nilsen, T. H. Flo, B. Fleckenstein, J. G. Iversen, T. Espevik, and B. Bogen. 2003. Cutting edge: link between innate and adaptive immunity: Toll-like receptor 2 internalizes antigen for presentation to $CD4^+$ T cells and could be an efficient vaccine target. *J. Immunol.* 171: 32–36.
54. Jackson, D. C., Y. F. Lau, T. Le, A. Suhrbier, G. Deliyannis, C. Cheers, C. Smith, W. Zeng, and L. E. Brown. 2004. A totally synthetic vaccine of generic structure that targets Toll-like receptor 2 on dendritic cells and promotes antibody or cytotoxic T cell responses. *Proc. Natl. Acad. Sci. USA* 101: 15440–15445.
55. Hart, J. P., M. D. Gunn, and S. V. Pizzo. 2004. A CD91-positive subset of $CD11c^+$ blood dendritic cells: characterization of the APC that functions to enhance adaptive immune responses against CD91-targeted antigens. *J. Immunol.* 172: 70–78.
56. Schjetne, K. W., H. T. Gundersen, J. G. Iversen, K. M. Thompson, and B. Bogen. 2003. Antibody-mediated delivery of antigen to chemokine receptors on antigen-presenting cells results in enhanced $CD4^+$ T cell responses. *Eur. J. Immunol.* 33: 3101–3108.
57. Biragyn, A., K. Tani, M. C. Grimm, S. Weeks, and L. W. Kwak. 1999. Genetic fusion of chemokines to a self tumor antigen induces protective, T-cell dependent antitumor immunity. *Nat. Biotechnol.* 17: 253–258.
58. Schjetne, K. W., K. M. Thompson, T. Aarvak, B. Fleckenstein, L. M. Sollid, and B. Bogen. 2002. A mouse C κ-specific T cell clone indicates that DC-SIGN is an efficient target for antibody-mediated delivery of T cell epitopes for MHC class II presentation. *Int. Immunol.* 14: 1423–1430.
59. Tacken, P. J., I. J. de Vries, K. Gijzen, B. Joosten, D. Wu, R. P. Rother, S. J. Faas, C. J. Punt, R. Torensma, G. J. Adema, and C. G. Figdor. 2005. Effective induction of naive and recall T-cell responses by targeting antigen to human dendritic cells via a humanized anti-DC-SIGN antibody. *Blood* 106: 1278–1285.
60. He, L. Z., V. Ramakrishna, J. E. Connolly, X. T. Wang, P. A. Smith, C. L. Jones, M. Valkova-Valchanova, A. Arunakumari, J. F. Treml, J. Goldstein, et al. 2004. A novel human cancer vaccine elicits cellular responses to the tumor-associated antigen, human chorionic gonadotropin β. *Clin. Cancer Res.* 10: 1920–1927.
61. Mahnke, K., Y. Qian, S. Fondel, J. Brueck, C. Becker, and A. H. Enk. 2005. Targeting of antigens to activated dendritic cells in vivo cures metastatic melanoma in mice. *Cancer Res.* 65: 7007–7012.
62. Bonifaz, L. C., D. P. Bonnyay, A. Charalambous, D. I. Darguste, S. Fujii, H. Soares, M. K. Brimnes, B. Moltedo, T. M. Moran, and R. M. Steinman. 2004. In vivo targeting of antigens to maturing dendritic cells via the DEC-205 receptor improves T cell vaccination. *J. Exp. Med.* 199: 815–824.